I&EC research
Industrial & Engineering Chemistry Research

Applied Chemistry

Engineered phosphate fertilisers with dual-release properties

Shervin Kabiri, Ivan B. Andelkovic, Rodrigo da Silva, Fien Degryse, Roslyn Baird, Ehsan Tavakkoli, Dusan Losic, and Michael J. McLaughlin

Ind. Eng. Chem. Res., **Just Accepted Manuscript** • DOI: 10.1021/acs.iecr.0c00403 • Publication Date (Web): 10 Mar 2020

is published by the American Chemical Society. 1155 Sixteenth Street N.W., Washington, DC 20036

Engineered phosphate fertilizers with dual-release properties

Shervin Kabiri[a, b*], Ivan B. Andelkovic[a, b*], Rodrigo C. da Silva[a], Fien Degryse[a], Roslyn Baird[a], Ehsan Tavakkoli[a,c,d], Dusan Losic[b] and Michael J. McLaughlin[a]

[a] Technology Research Centre, School of Agriculture, Food and Wine, The University of Adelaide, PMB 1, Waite Campus, Glen Osmond, SA 5064, Australia

[b] School of Chemical Engineering, The University of Adelaide, Adelaide, SA 5005, Australia

[c] NSW Department of Primary Industries, Wagga Wagga Agricultural Institute, Wagga Wagga, NSW 2650, Australia

[d] Graham Centre for Agricultural Innovation, Charles Sturt University, Wagga Wagga, NSW 2650, Australia

Corresponding authors:

*ivan.andelkovic@adelaide.edu.au; +61 8 8313 2879

*shervin.kabiri@adelaide.edu.au; +61 8 8313 3093

Abstract

A new strategy to produce phosphate (P) fertilizers with both fast and slowly soluble P by compaction method to produce composite products is presented. This unique composition is created by combining mono-ammonium phosphate (MAP) as a highly soluble P nutrient source, with a commercially available slow-release P such as struvite (Str) or P-loaded graphene oxide (GO). Graphene oxide-loaded P was synthesized by *in situ* oxidation of GO and ferrous ion (GO-Fe) mixtures with hydrogen peroxide and further loading of P onto the GO-Fe composite. Nutrient release in water was studied for dual-release MAP-Str and MAP-GO-Fe-P and compared to their corresponding slow and fast release sources. Column perfusion experiments showed a biphasic dissolution behaviour with no significant difference between MAP-GO-Fe-P and MAP-Str. Visualization of P diffusion and chemical analysis of the soil after diffusion was used to assess the diffusion of P from different P fertilizers in various types of soil. Runoff and leaching simulations were performed to investigate the effects of the prepared fertilizer formulations on the environment. Overall, the diffusion of the dual-release fertilizers and the P loss in runoff and leaching experiments was less than for MAP. The better environmental performance of the dual-release fertilizers compared to MAP was related to the specific properties of the GO-based materials such their two-dimensional structure and to the low solubility of the Str in the case of Str-based fertilizers.

Introduction

Substantial efforts are now being made to improve fertilizer efficiency yet environmental and economic issues related to fertilizer usage still exist. The current application of highly soluble P fertilizers possesses a high risk of leaching and/or runoff of P into water systems which can trigger serious environmental problems.[1, 2] Previous studies have identified P fertilizers as the main provider of P to surface water bodies contributing to their pollution.[3] Depending on the site conditions, type and application rate of P fertilizers, fertilizer placement practice and timing of fertilizer application with respect to rainfall, the P losses usually result from a combination of surface runoff of particulate or dissolved P, channelized surface runoff, drainage and/or groundwater transport.[2] Furthermore, significant P leaching can occur in sandy soils resulting in P deficiency due to the low P retention and high hydraulic conductivity.[4]

Most studies have confirmed that the environmental risk associated with P fertilizers such as surface runoff or leaching is due to a combination of the high solubility of most commonly used P fertilizers such as monoammonium phosphate (MAP) and diammonium phosphate (DAP), as well as climatic or management conditions that lead to surface water runoff.[3, 5, 6] Phosphorus fertilizers with slow-release properties can help mitigate the high losses of P encountered when high intensity rainfall or irrigation occurs shortly after surface applications.[7, 8]A conventional approach for the synthesis of slow-release fertilizers (SRFs) is by coating the soluble fertilizer to create a physical barrier around the granule which can decrease the release rate of the nutrients.[9] Materials used for the coatings are usually cheap, readily available, biodegradable and/or environmentally friendly, either natural[10, 11] or synthetic polymers.[12-14] However, the synthesis of most synthetic polymers requires organic solvents which are harmful and expensive.[15] Moreover, the polymer coatings often have low biodegradability and could potentially become an environmental concern.[16, 17]Other strategies included the use of sparingly soluble materials, such as hydroxyapatite,[18] struvite,[19] or different types of phosphate rock,[20] as well as usage of various natural and synthetic materials like layer-double hydroxides (LDH),[21, 22] silicates [23] and GO[24] as nutrient carriers.

The idea underpinning the application of SRFs is based on an assumption that gradual supply of P to the plant will reduce the immediate and large nutrient losses due to leaching/runoff of P immediately after fertilizer application, while matching the plant P requirement for a longer period of supply during the growing season for slower-growing crops in cooler climates.[9, 25] While the application of low solubility fertilizers can decrease the risk of P leaching/runoff, [3] reduced agronomic effectiveness might occur due to the slower supply of P during periods of peak plant demand.[19, 21] For instance, P uptake by spring wheat was significantly lower for granular Str-based P fertilizer compared to MAP in both acidic and alkaline soils.[19] Other studies have found sparingly soluble P fertilizers to

have similar agronomic effectiveness to soluble P fertilizers, but often these studies used fine particles mixed through the soil, which enhances the dissolution of the sparingly soluble product.[19, 26-28] Everaert et al.[21] reported considerably higher P uptake by plants treated with MAP compared to slow-release LDH or Str fertilizer treatments. Their study also indicated that MAP performed better than Str and LDH in alkaline soil even when Str was applied in powdered form. Another study conducted with GO-based P carriers showed the inefficiency of the slow-release P fertilizers for wheat growth and P uptake compared with highly soluble MAP. [29]

Management practices, in particular timing, rate and placement, have a very large effect on fertilizer runoff losses, especially in soil erosion. However, best management practices are not always followed due to logistic constraints. Improving fertilizer formulations can reduce nutrient losses in runoff water when fertilizers are surface applied. Recently, da Silva et al.[30] have found that the combination of fast- and slow-release boron (B) fertilizers in macronutrient (muriate of potash) fertilizers can enhance the efficiency of B fertilizers. The combination of the fast- and slow-release B resulted in the initial fast-release of B followed by a sustained release of B for a longer time.[30] They have also reported a reduced risk of B loss during a leaching experiment. Therefore, the same concept can be applied for P fertilizers to combine fast- and slow-release P sources to obtain a product with dual-release properties which reduces losses of P in runoff (or leaching) while also not severely compromising agronomic effectiveness of the fertilizer.

In our previous studies,[24, 31] we showed that graphene composites can be used as an excellent carrier for nutrients providing very slow and controllable release of micronutrients or P. Considering that graphene structure, surface chemistry, nutrient loading and release characteristics are tuneable, it presents a very promising platform for designing the next generation of fertilizers with controlled nutrient release kinetics. A serious limitation of preparing graphene-P composites is maintaining low pH during synthesis to avoid hydrolysis of Fe^{3+} ions during loading onto the GO suspension. Considering that Fe^{3+} ions have a high affinity towards oxygen groups present at the surface of GO, the high concentration of protons at low pH suppresses the deprotonation of carboxyl groups at the edge of GO sheets and cause a dramatic decrease of the negative charge on the GO sheets surface, and hence reduces the loading capacity of Fe and subsequently loading of P.[32, 33] Low P content fertilizers cost more to transport and to spread, so we first aimed to increase the P content of the GO composite. We therefore hypothesized that mixing a GO suspension with Fe^{2+} salts at pH values > 2 followed by *in situ* oxidation using H_2O_2 could increase the number of carboxyl groups at the edge of GO, increasing the overall negative charge while simultaneously complexing generated Fe^{+3} ions. This procedure should improve the loading of Fe^{3+} and subsequently PO_4^{3-} ions on the GO sheets.

Therefore, the first objective of this work was to synthesize GO-Fe loaded P composites with higher P loading capacities which could be used as slow-release sources of P.

Another objective of this study was to develop P fertilizers with dual release properties, releasing less P immediately after application and having a more sustained and longer period of P release than current soluble P sources. Two sources of slow-release P, namely a P-loaded graphene-oxide or struvite, were co-compacted with a highly soluble P source, with the aim of creating fertilizers with dual release properties. We hypothesized that a dual-release fertilizer will reduce the overall dissolution rate and the diffusion of P in water and soil compared to conventional MAP thus potentially reducing the environmental issues related to large runoff or leaching losses of P immediately after fertilizer application.

Experimental section

Natural graphite flakes were sourced from a local mine (Eyre Peninsula, South Australia). Ferrous sulphate ($FeSO_4$ $7H_2O$, Sigma-Aldrich), potassium permanganate ($KMnO_4$, Sigma-Aldrich), potassium dihydrogen phosphate (KH_2PO_4, Chem-Supply), sulphuric acid (98 %, H_2SO_4, Chem-Supply), phosphoric acid (85 % w/w, H_3PO_4, Chem-Supply), hydrogen peroxide (30 %, H_2O_2, Chem-Supply), hydrochloric acid (35 %, HCl, Chem-Supply), and ethanol (Chem-Supply) were used directly without further purification. Struvite (Crystal Green™, (SGN240)) and MAP were supplied by (Ostara Nutrient Recovery Technologies Inc, Vancouver, BC and Mosaic Co, Plymouth, MN), respectively.

GO-Fe composite preparation

The GO sheets were prepared using a modified Hummer method.[34] To prepare GO-Fe composites, approximately 200 mg of GO was ultrasonicated in 20 mL of deionized water to obtain a homogeneous dispersion while the pH was adjusted to 3. Then, 1 g of ferrous sulphate was dissolved in a minimum amount of deionized water and added to the GO, under vigorous stirring, to provide GO:Fe ratio of 1:1 (g/g). Subsequently, 2 mL of H_2O_2 was added in 0.2 mL portions (to avoid violent reaction) to the GO-Fe mixture at ~1 min time intervals. The mixture was stirred for 1 h and then centrifuged at 2950*g* (Thermo Scientific Sorval, H-6000B rotor) for 1 h. After centrifugation, the supernatant was removed, and the GO-3Fe composite was freeze dried. Following the same procedure, GO-4Fe and GO-5Fe composites, with initial pH of GO suspensions of 4 and 5, respectively, were also synthesized. Henceforth, GO-XFe notation is used, where X denotes the initial pH value of the GO suspension used for synthesis.

Loading of P onto GO-Fe composite

For loading of P onto the GO-3Fe composite, potassium dihydrogen phosphate (KH_2PO_4) salt was used as a source of soluble P. The GO-3Fe composite was suspended in deionized water at a concentration of 10 mg mL^{-1} and the pH was adjusted to 6 using NaOH. Then, KH_2PO_4 salt was added, under vigorous stirring in order to achieve a GO-3Fe:P ratio of 1:0.5 (g/g) and mixed for 1 h. The dispersion was centrifuged at 2950*g* for 1 h. After centrifugation, the supernatant was removed and the GO-3Fe composite loaded with phosphate (GO-3Fe-P) was freeze-dried. The dried composite was homogenized using a mortar and pestle and pressed into 40 mg pellets using a desktop pill presser (TDP 5, LFA Machines Oxford Ltd, UK). The same procedure was used for loading of P onto the GO-4Fe and GO-5Fe composites. Loading experiments were done in duplicate.

The total amount of elements in GO-Fe-P composites

The total concentration of elements (Fe, K, P and S) in the GO-3Fe-P, GO4Fe-P, and GO-5Fe-P samples were determined using an open vessel concentrated acid digestion procedure (3.75: 1.25: 1 mL of concentrated HCl: HNO_3: $HClO_4$).[35] The samples (~0.1 g) were added into a glass tube with 6 mL of a mixture of concentrated acids and digested on a heating block at 140 °C for 6 h. After digestion, samples were filtered using 0.45 µm syringe filters (Sartorius) and analysed for total elemental concentrations using Inductively Coupled Plasma-Optical Emission Spectroscopy (ICP-OES) (Spectro, Kleve, Germany). Acid digests were performed in triplicate.

Preparation of fertilizers formulations

Five fertilizer formulations were chosen for this study (Table 1): a commercial MAP fertilizer, a commercial Str fertilizer, a synthesized GO-Fe-P fertilizer, a mixture of Str with MAP and a mixture of GO-Fe-P with MAP (the GO-Fe-P fertilizer synthesized at pH 3 was used). The dual release fertilizers were made by mixing MAP powder (< 250 µm) and either Str (< 250 µm) or GO-Fe-P powder in a ratio that provided 50% of P from MAP and 50% from the slow-release fertilizer source. The freeze-dried GO-Fe-P powder and the dual release mixtures were homogenized using a mortar and pestle and pressed into 40-mg pellets using a desktop pill presser (TDP 5, LFA Machines Oxford Ltd, UK).

The pH of the product was determined by shaking 1 g of fertilizer in 2 L of water for 2 h. The total composition of MAP, Str and MAP-Str was measured by acid dissolution in 3.2 M HNO_3, followed by analysis using ICP-OES.

Table 1. pH, water extractable P, and total P, Mg, Fe, S and K concentrations (weight %) for monoammonium phosphate (MAP), struvite (Str), graphene oxide-loaded iron and phosphorus (GO-3Fe-P), dual-release MAP-Str and MAP-GO-3Fe-P. The numbers in brackets refer to the standard deviation of three measurements.

Fertilizer	pH	Water extractable P (g kg^{-1})	Total (g kg^{-1})				
			P	Mg	Fe	S	K
MAP[a]	5.6(0.1)	192 (2)	227 (5)	5 (1)	ND	14 (0)	ND
Struvite[b]	7.5(0.1)	4.3 (0.2)	122 (1)	100 (2)	ND	ND	ND
GO-Fe-P	6.7(0.0)	32 (1)	140 (6)	ND	152 (2)	9 (1)	142 (7)
MAP-Str	6.9(0.0)	83 (1)	158 (13)	81 (1)	6 (0)	7 (1)	15 (0)
MAP-GO-3Fe-P	6.0(0.0)	91 (6)	173 (5)	5 (0)	106 (2)	13 (0)	94 (3)

[a] Commercial monoammonium phosphate fertilizer

[b] Commercial struvite fertilizer

ND refers to not detected in the samples

Dissolution kinetics of P

A column dissolution experiment was performed to quantify the kinetics of P release from MAP, GO-3Fe-P, Str, MAP-GO-3Fe-P and MAP-Str using the method of Baird et al. (2019).[36] Briefly, granules of individual formulations having a total amount of P equivalent to ~50 mg were placed in a polypropylene column (150 mm×15 mm) and the column filled with acid-washed glass wool. Deionized water was introduced from the bottom of the column using a peristatic pump at a constant flow rate (10 mL h^{-1}). The eluate containing dissolved nutrient was collected using an automated fraction collector (SuperFracTM, Pharmacia) for 48 h. The concentration of P was determined by ICP-OES. All treatments were carried out in duplicate.

Soils

Two soils from southern Australia were used. They were collected from near Monarto (MO) and Mt Compass (MC) from the top layer (0–10 cm), air dried, sieved to <2 mm, and thoroughly mixed prior to characterization and use. Selected physical and chemical properties of the soils used are given in Table 2. Soil pH was determined in 0.01 M $CaCl_2$. Total C was determined using a dry combustion method.[37] A pressure calcimeter method was used to determine the content of $CaCO_3$.[38] Particle size was measured according to the procedure of McKenzie et al (2002).[39] The cation exchange capacity (CEC) at pH 7.0 and oxalate-extractable Al and Fe concentrations were determined following Rayment and Higginson. [40]

Table 2. Selected physical and chemical properties of the soils used in this study.

Soil	Monarto	Mt Compass

pH (water)	7.5	5.9
pH ($CaCl_2$)	7.0	4.9
OC (g kg^{-1})	10	5
CEC ($cmol_c$ kg^{-1})	8.2	2.0
Clay (%)	8.6	4.2
Silt (%)	7.4	0.9
Sand (%)	84.0	94.9
$CaCO_3$ (g kg^{-1})	< 2	< 2
Fe_{oxal} (mg kg^{-1})	236	138
Al_{oxal} (mg kg^{-1})	345	38
Total P (mg kg^{-1})	107	20

Diffusion of P from fertilizer granules into soil

A Petri dish experiment was carried out in which the diffusion of P from the dual-release (MAP-Str and MAP-GO-3Fe-P) formulations was assessed and compared to that from the soluble fertilizer (MAP) or slow-release formulations (Str or GO-3Fe-P). The two soils were wetted to the field capacity and Petri dishes (diameter of 5.5 cm) were filled with the moist soil. One granule of each formulation (MAP, GO-3Fe-P, MAP-Str, MAP-GO-3Fe-P or Str) containing 8 mg P was placed in a 5-mm deep hole in the centre of the dish. The hole was then carefully covered with soil and Petri dishes were incubated at 25 °C. Each treatment was replicated three times. The diffusion of P was visualized at 1, 3, 7, 14 and 28 d after fertilizer application using Fe-oxide impregnated paper according to the method of Degryse and McLaughlin. [41]

The total amounts of P extracted by acid were measured at the end of the incubation period for two concentric soil sections following the method described by Lombi et al.[42] Soil samples from the inner and outer sections (<8 mm and >8 mm from the fertilizer application point) were homogenized after drying in the oven overnight. To measure the total amount of P, a 10 mL solution containing 20% HNO_3 was added to 0.2 g of soil from the inner or outer sections. The suspensions were shaken overnight and centrifuged 2950 g prior to measuring P with ICP-OES.

Runoff experiment

A rainfall simulation experiment was performed in the laboratory using a rainfall cabin similar to Everaert et al.[3] Briefly, three runoff trays (with dimensions of 50-cm length, 20-cm width and 7.5-

cm depth) were placed 1 m under a spray nozzle while a runoff collector was attached to their front section. The runoff tray collector sections were covered to prevent the dilution of runoff solution by direct rainfall. The rainfall set up was pre-calibrated to the rainfall intensity of 98 mm h^{-1} for the experiment.

The runoff trays were filled with MO soil up to the lower lip of the tray and to achieve a bulk density of 1.4 g mL^{-1}. Perennial ryegrass (*Lolium perenne L.*) was planted in the soil for vegetation cover and all trays were located in the glasshouse. The trays were watered regularly and grass growth was monitored. The grass was cut to a height of 5 cm after 2 wk to promote root establishment. It was cut after another 14 d to the same height and 1 d later the P fertilizers MAP, GO-3Fe-P, Str, MAP-GO-3Fe-P or MAP-Str were applied onto the surface of runoff trays at a rate equivalent to 40 kg P ha^{-1} (0.4 g P $tray^{-1}$). A control treatment was prepared without addition of fertilizer. Runoff was generated at 1, 3, 7, 14 and 21 d after the fertilizer application by exposing the trays to the calibrated water spray. Tap water was used in the rainfall simulator, the P concentration of which was below the detection limit of the ICP-OES (0.004 mg L^{-1}), other elements detected in tap water are summarized in Table S1. For all rainfall events, the water was collected from the trays continuously for 30 minutes after the first droplets of runoff water were generated. Day 1 runoff water was collected separately for 30 minutes in time intervals of 0 to 5, 5 to 15, and 15 to 30 min, whereas for the rest of the rainfall events, water was continuously collected from 0 to 30 min. The weight of the runoff water was recorded for each tray. The runoff water was filtered through a 0.45 µm filter before analysis with ICP–OES.

Soil leaching experiment

A column leaching experiment was conducted to evaluate the leaching of P from soils treated with the MAP, GO-3Fe-P, Str, MAP-GO-3Fe-P, and MAP-Str fertilizers, using 50-ml plastic syringes as columns. The bottom of the columns were covered with a 1.5-mm layer of glass wool to prevent movement of soil particles. Then, 25 g of dry MC soil was added, fertilizer granules were added at a rate of 60 mg P per column and covered with 25 g of MC soil. The columns were incubated at 25 °C. Aliquots of 30 mL of water were introduced from the top of the column at time intervals of 1, 3, 7, 15, 21 and 28 d after addition of fertilizers and collected from the bottom, using a syringe to create suction. The leachates were filtered with a 0.45 µm filter and P concentrations determined using ICP-OES.

Kinetic models

The mechanism of P release from all formulations was described and interpreted using different kinetic models, known as the zero- (eq.1), first-order(eq.2) and Higuchi (eq.3) models.[43, 44]

$$\frac{q_t}{q_e} = K_0 t \quad (1)$$

$$log(q_e - q_t) = log(q_e) - K1\left(\frac{t}{2.303}\right) \quad (2)$$

$$q_t = k_h t^{0.5} \quad (3)$$

Where q_t and q_e represent the amount of nutrients released at time t and equilibrium, respectively, and K_0, K1 and k_h are solubility rate constants.

Characterization

The GO-Fe-P samples synthesized at pH 3, 4 and 5 were fully characterized. Thermal decomposition of samples was performed under air using a thermogravimetric analyser (Q500, TA Instruments, USA) heating from room temperature to 900 °C at a rate of 10 °C/min. X-ray diffraction (Model Miniflex 600, Rigaku, Japan) measurements were performed from 2θ = 5°–80° at a scan rate of 5°/min. FTIR (Nicolet 6700 Thermo Fisher) was used to identify functional groups in materials by scanning in the range of 500–4000 cm^{-1} in transmission mode. Scanning electron microscopy (SEM, Quanta 450, FEI, USA) was used to investigate the morphology of the fertilizer granules. The AFM image of GO was obtained on a multimode scanning probe microscope equipped with a Nanoscope IIIa controller (Vecco, USA).

Data Analysis

Analysis of variance (ANOVA) was performed using IBM SPSS statistical software. Multiple comparison of means was conducted using the LSD test when the ANOVA indicated significant differences. The level of significance was set at P≤0.05.

Results and discussion

Characterization

The XRD profile of GO (Fig. 1a) showed a characteristic peak for GO at 2θ = 10.4˚, corresponding to the (002) reflection.[45] Disappearance of this diffraction peak in the XRD profile of GO-Fe composite synthesized at pH 3 (Fig. 1a) indicates a loss of the stacked structure of GO sheets, due to the introduction of Fe^{3+} ions among the GO layers, as well as lack of formation of any iron crystal structures on the surface of the GO.[46] The absence of the diffraction peak at 10.4˚ for the GO-3Fe-P composites further points out that no crystalline phase was produced on the GO-3Fe composite during the loading of PO_4^{3-} onto GO-3Fe.[24, 47] Similar XRD patterns to GO-3Fe and GO-3Fe-P were obtained for GO-XFe and GO-XFe-P composites synthesized at pH 4 and 5 (Fig. S1).

Interactions between GO functional groups, Fe^{3+} and PO_4^{3-} ions were examined using FTIR. The FTIR spectra of GO exhibits a broad band between 2100 to 3650 cm^{-1} for O-H stretching vibration due

to the intercalated water and structural hydroxide groups (-COOH, and –COH) of GO.[34, 48, 49] The peak at 1712 cm^{-1} corresponds to C=O stretching of –COOH, and peak at 1618 can be allocated to C=C skeletal vibrations of the non-oxidized graphitic structure. Meanwhile, peaks at 1030 cm^{-1} and 1213 cm^{-1} conform to the C-O and C-OH bonds, respectively. [34, 50-54] As illustrated in Fig. 1b, addition of Fe^{2+} ions and H_2O_2 to the GO suspension at an initial pH value of 3 resulted in a significant decrease of the 1730 cm^{-1} peak and a shift of the 1618 cm^{-1} (to 1614 cm^{-1}) and 1220 cm^{-1} (to 1187 cm^{-1}) peaks, corresponding to carboxylic, aromatic and epoxy stretches in GO, respectively.[55] These experimental results demonstrate the interaction of Fe ions with the O functional groups and the π-π aromatic structure of GO. The new peak at 588 cm^{-1} of the GO-Fe composite can be attributed to the Fe-O bond, further indicating the iron loading onto the GO sheets.[55] A strong stretching band at 1008 cm^{-1} after loading of PO_4^{3-} ions onto the GO-Fe composite could be assigned to deprotonated monodentate surface complex P-OX (where X is either H or Fe).[56] Composites obtained at other pH values resulted in identical FTIR spectra (Fig. S2), suggesting that there is no difference in loading mechanisms onto GO in the tested pH range (3-5).

TGA analysis of GO, GO-3Fe and GO-3Fe-P is shown in Fig. 1c. Weight loss up to 100° C could be attributed to detachment of physically adsorbed water, followed by another loss of weight in the range 200-600° C due to decomposition of labile oxygenated functional groups and subsequent decomposition of the carbon structure.[57, 58] At temperatures higher than 600° C, no change in weight was observed for GO and GO-3Fe, and undegradable solid residues were 2.6 and 33.5 wt % for GO and GO-3Fe, respectively. Based on the TGA results, the loading of iron onto the GO-3Fe composite was calculated to be 21.6 wt %. It is interesting to notice lack of significant weight loss for the GO-3Fe-P composite, compared to GO and GO-3Fe, in the 400 to 900° C temperature range. Increased thermal stability of the GO-3Fe-P composite could be ascribed to the formation of ferric phosphate complexes which have temperatures of decomposition greater than those used in our experiments.[59] Similar results were obtained for composites synthesized at pH 4 and 5 (Fig. S3). It is well known that the surface charge of GO at pH 3 is negative and further increase of pH to 5 will only slightly change zeta potential towards more negative values.[60, 61] Based on our results these slight changes do not have a significant impact on the mechanism and amount of Fe loaded at the GO surface.

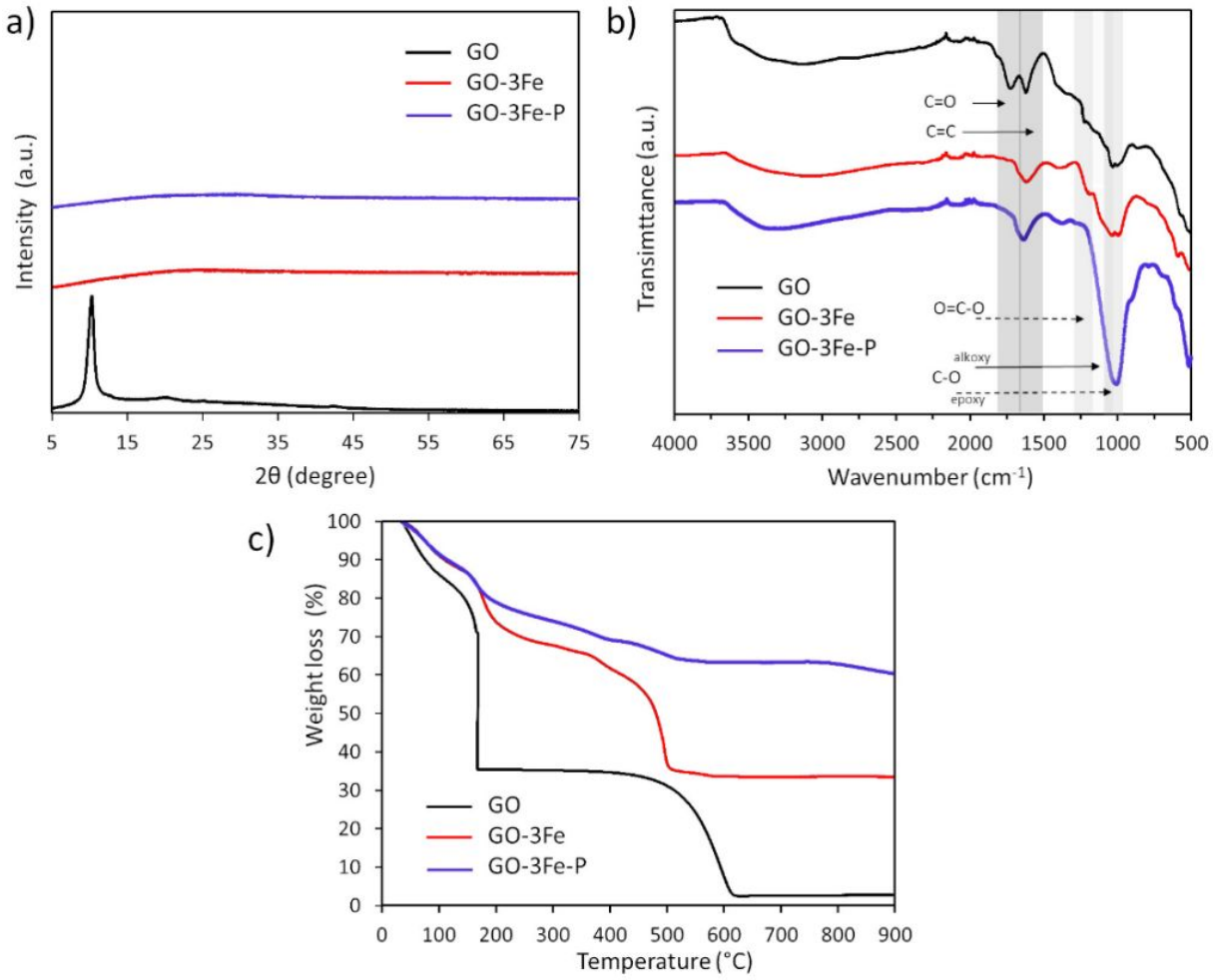

Figure 1. a) X-ray diffraction spectra, b) FTIR spectra and c) TGA analysis of graphene oxide (GO), graphene oxide loaded with iron in pH 3 (GO-3Fe) and graphene oxide loaded with iron and phosphorus (GO-3Fe-P).

The analysis of GO-XFe-P composites after acid digestion using ICP-OES showed that the difference in the amounts of P, K, S and Fe in the GO-XFe-P composites were less than 1% indicating a negligible effect of pH on elemental loading (data not shown). This is in accordance with the characterization results which showed an identical mechanism of interactions for all the three pH values. The presence of sulphur (S) could be explained by the adsorption of SO_4^{2-} ions from the $FeSO_4$ salt, used as a source of Fe, onto the GO-3Fe composite. Likewise, the addition of KH_2PO_4 salt as a source of P during synthesis of the GO-3Fe-P composite resulted in sorption of potassium (K^+) ions. The relatively large percentage of Fe in the GO-3Fe-P composite is most likely the reason for the high loading of P, due to the high affinity of PO_4^{3-} towards Fe^{+3} ions.[31] The presence of K in the GO-3Fe-P composite may be the result of electrostatic attraction of K^+ ions with negatively charged oxygen groups and PO_4^{3-} groups on the surface of the GO-3Fe-P composite. The small percentage of S present on the GO-3Fe-P could be attributed to the fact that SO_4^{2-} competes for the same Fe sites as PO_4^{3-} and has a lower affinity for the surface than PO_4^{3-}.[62, 63]

Analysis of the composites, obtained by the simultaneous addition of Fe^{2+} and H_2O_2 at a pH > 2 to the GO suspension in water, had high concentrations of iron attached to the oxygen groups of the GO sheets. Furthermore, Zhang et al. [33] reported that treatment of GO suspensions in water using $FeSO_4x7H_2O$ followed by addition of H_2O_2 would generate Fe(III) composites linked to the GO sheet edges or surface. Characterization of GO-XFe composites loaded with P suggests the formation of ferric phosphate complexes at the surface of GO-XFe. The amount of P and K loaded onto the GO-XFe-P composites were close to the values found in typical commercial fertilizers. Based on our previous work,[31] all these newly synthesized composites were expected to behave as SRFs. The GO-3Fe-P (further labelled as GO-Fe-P) composite was chosen as the model slow-release P source for co-compaction with MAP.

Kinetics of phosphorus release

The kinetics of P dissolution from fertilizers are reported as the cumulative amount of P eluted from the column versus time (Fig. 2a). The overall release behaviour depended on the solubility of the fertilizers. Those with the higher water solubility showed faster P release e.g. the P release for MAP fertilizer was very fast with 90% of the added P eluted in the first 10 h. For the slow-release fertilizers (Str and GO-Fe-P), only 10% of the P was measured in the leachate in the first 10 h, and Str showed a slower release compared to GO-Fe-P for the next 40 h. The release of P for both fertilizers containing high and low water soluble P sources showed a biphasic behaviour consisting of an initial release in the first 10 h, followed by a slow release over the next 40 h. The release of other nutrients such as K and S was also monitored from GO-Fe-P and is reported in Supporting Information (Fig. S4).

The pH of eluates from MAP fertilizers increased from 5.5 to 6.5 for the first 15 h when 90% of P released and once the dissolution of the granules was completed, the column eluate tended towards a pH value of 6, corresponding to the eluent pH (Fig. 2b).[31] The pH of eluates from the GO-Fe-P fertilizers decreased to 5.5 for the first 10 h and maintained this pH throughout the elution study. This decrease of pH was most likely caused by the production of H^+ ions during the dissolution of the GO-Fe-P composite, [31] as GO can gradually generate acidity by interaction with water.[64] In contrast, the pH of the initial eluates from the columns containing Str was 7.5. The pH of eluates from the MAP-GO-Fe-P and MAP-Str demonstrated similar trends to MAP for the first 15 h and then increased from 6 to 6.5 and 7 for MAP-GO-Fe-P and MAP-Str, respectively. Once the dissolution of the MAP was complete, the pH of the eluates from MAP-GO-Fe-P remained around 6.5, while the pH of eluates from MAP-Str tended towards higher pH (around 7.5) due to dissolution of Str.

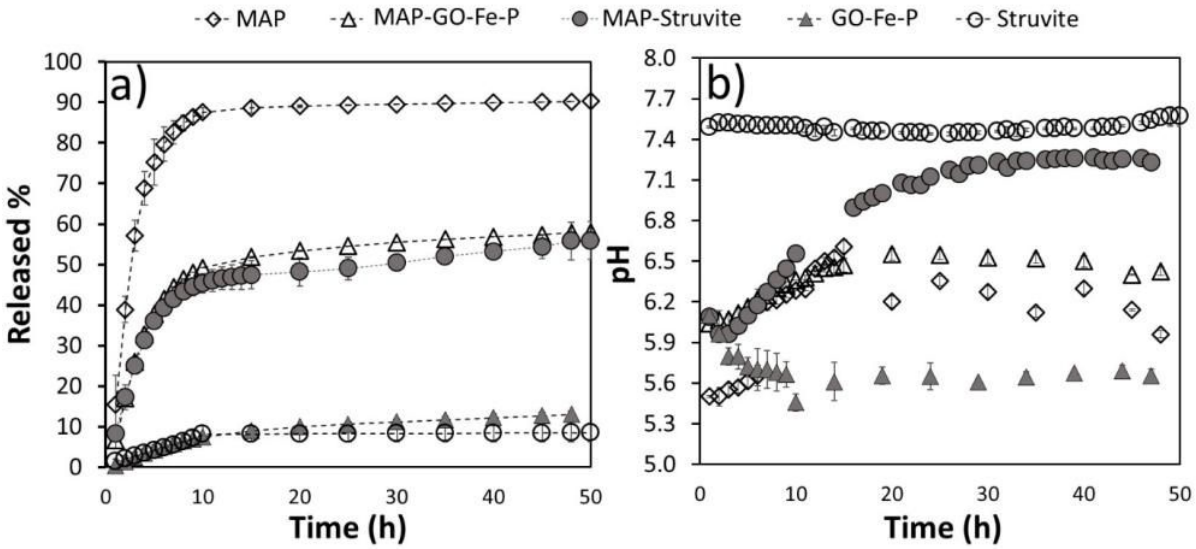

Figure 2. a) Kinetics of P release from monoammonium phosphate (MAP), graphene oxide loaded P (GO-Fe-P), struvite (Str), MAP mixed GO-Fe-P (MAP-GO-Fe-P) and struvite (MAP-Str) from the columns and b) Changes in the pH of the eluates from the columns as a function of time. Error bars represent standard deviation (n=2).

There was no Fe detected (< 10 µg L^{-1}) in the eluates of the GO-Fe-P composite, indicating that only P, not Fe, was released. The slow release of P observed from GO-Fe-P fertilizers could be related to the strong complexation of P with the Fe-loaded GO.[31] Another reason for slow release of P from the GO-based matrix is the low accessibility of nutrients in the matrix due to the trapping of P in or between GO sheets. Coordination of Fe on GO and subsequently P on GO-Fe creates wrinkles on the GO surface due to its decreasing surface charge.[31, 65] Therefore, nutrients can be trapped in GO aggregates and water molecules have to penetrate through the agglomerated GO sheets to release the nutrient.[24] The slow release of Str was due to the low solubility of the mineral which is mostly governed by the activity of Mg^{2+}, NH^{4+}, and PO_4^{3-} in solution and strongly depends on the pH of the solution.[66]

The kinetic constant (k) for the release behaviour and the release concentration of P from MAP, Str and GO-Fe-P at equilibrium time were fitted using the linear form of zero-order, first-order and Higuchi models (or intraparticle diffusion model) (Table 3). The data for MAP fitted the first order model best. Conforming to this kinetic model, the rate of P released from the MAP granules is directly proportional to the initial concentration of P.[44] In contrast, the P release constant and the regression coefficient (R^2) data presented in Table 3 showed that the P release from the GO-Fe-P and Str was best described using the Higuchi model. This model was developed to model the release of low solubility nutrients incorporated into semi-solid or solid matrices, hence similar to a material such as P-loaded GO.[44] Therefore, water needs to diffuse inside the matrix and release the nutrient through the cracks on the

granule's surface. A SEM image of Str and GO-Fe-P granules (Fig. S5) confirmed this as granules were corrugated with cracks but their structure appeared firm.

Table 3. Kinetic pseudo-first and second- order, and Higuchi models for P release from MAP, Str and GO-Fe-P.

Kinetic parameters / Sample Name	Zero-order model		First-order model		Higuchi model	
	K_0 (h^{-1})	R^2	K_1 (h^{-1})	R^2	K_h (mg (g $h^{0.5}$)$^{-1}$)	R^2
MAP	-0.7605	0.3379	0.1087	0.7926	12.5990	0.5714
Struvite	-0.1206	0.5826	0.0918	0.6720	0.9873	0.7580
GO-Fe-P	-0.2787	0.8468	0.0644	0.9540	0.3240	0.9580

The dual-release P fertilizers showed two release patterns: a fast release for the first 10 h followed by a slow- and sustained release. Indeed, ~45% of the total P released from both MAP-GO-Fe-P and MOP-Str in the first 10 h, while it took 38 h more to reach the 56% release for total P. The slightly higher dissolution of P for MAP-GO-Fe-P compared to MAP-Str during the sustained release period could be related to the high pH of MAP-Str restricting P dissolution from Str. The release data of MAP-Str and MAP-GO-Fe-P were fitted to different kinetic models where initial and slow release data were fitted separately to the models. Initial and slow release data of MAP-Str and MAP-GO-Fe-P fitted the first-order kinetic model well which suggests that the P release rate is concentration dependent, related to P release from MAP (Table 4) and declined when all P from MAP was released. The release of P from MAP-Str and MAP-GO-Fe-P was also fitted to the Higuchi model, which is used to summarize the release of high and low solubility nutrient compounds merged into solid or semi-solid matrices. This model has used to describe the drug release by diffusion in the case of some matrix tablets containing water-soluble drugs the same condition as MAP-Str and MAP-GO-Fe-P granules. [67, 68]The Higuchi model also described the release of slow-release Str and MAP-GO-P well. The kinetic rate constant (K_1 and K_h) data calculated for P release for both dual-release fertilizers were greater for the first step (fast release) than the second step (slow release), confirming the faster release of MAP compared to slow-release sources.

Table 4. Comparison of release constants and co-relation factors for burst and sustained release obtained by fitting the P release data to zero- and first- order, and Higuchi models for MAP-Str, and MAP-GO-Fe-P.

Kinetic parameters	Zero-order model				First-order model				Higuchi model			
	K_0 (h^{-1})		R^2		K_1 (h^{-1})		R^2		K_h (mg (g $h^{0.5}$)$^{-1}$)		R^2	
	1° step	2° step	1° step	2° step	1° step	2° step	1° step	2° step	1° step	2° step	1° step	2° step
MAP-Str	3.935	1.025	0.890	0.944	0.177	0.042	0.982	0.997	16.119	12.366	0.971	0.964
MAP-GO-Fe-P	4.495	1.159	0.896	0.947	0.201	0.045	0.993	0.995	17.743	15.118	0.964	0.990

Runoff losses

As expected, runoff losses were very low for the Str and GO-Fe-P treatments; in the case of Str being not significantly different from soluble P losses from control (unfertilized) soil (Fig. 3). Runoff losses of P from MAP were high initially (as expected) and declined rapidly over time (Fig. 3a and b). The dual release sources had runoff losses of P intermediate between the highly soluble MAP, and the slow release sources, Str and GO-Fe-P. This is also reflected in the cumulative P loss data (Fig. 4). Compared to MAP, it was evident that the dual release sources reduced the initial flush of soluble P lost in the first rainfall event, particularly the one based on GO-Fe-P as the slow release source (Fig. 3a). The results of other studies have also shown that less water soluble P fertilizers resulted in a lower concentration of P in runoff than highly soluble P fertilizers. [69]

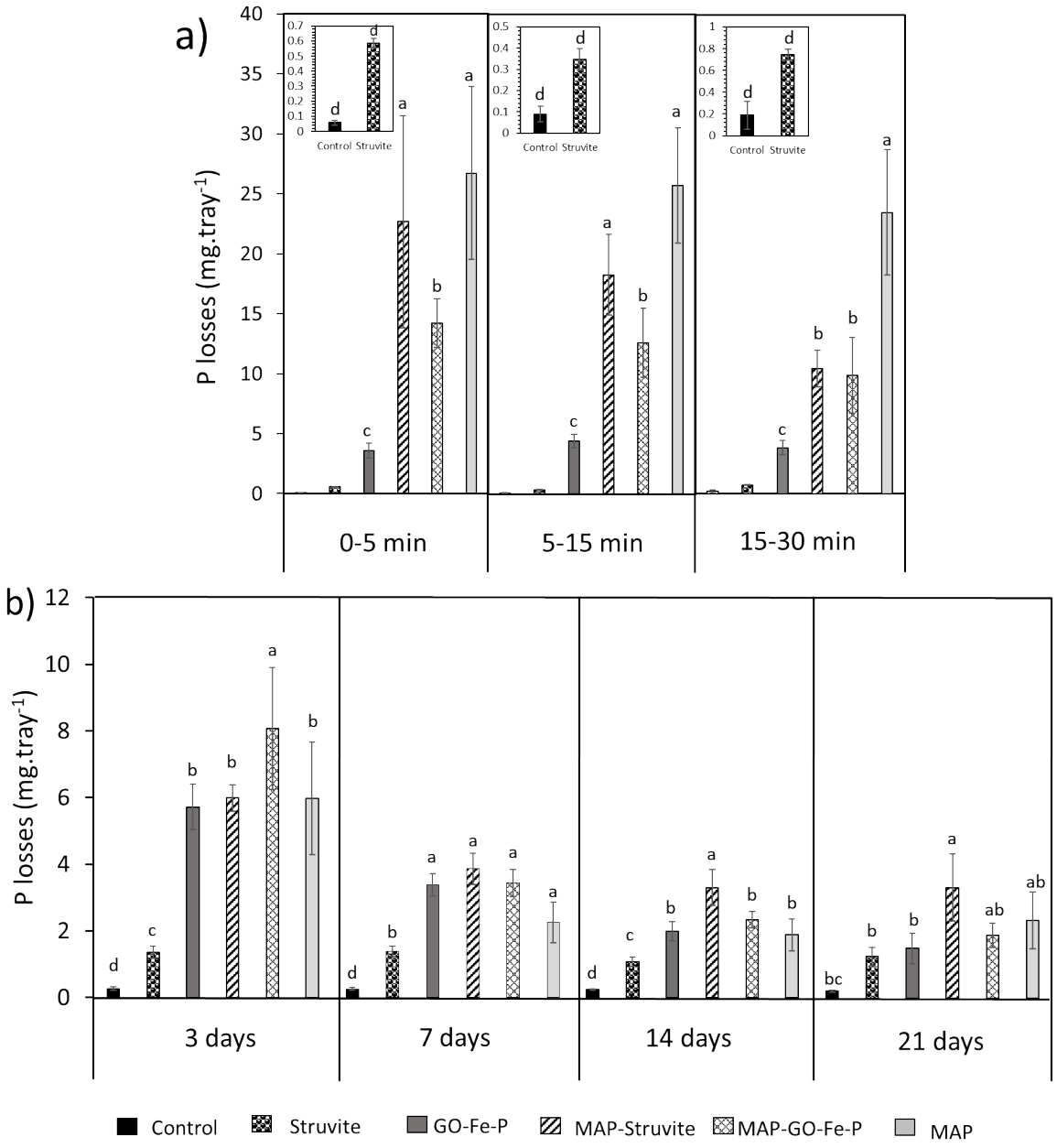

Figure 3. a) The runoff losses of dissolved P from MAP, GO-Fe-P, MAP-GO-Fe-P and MAP-Str and struvite during the time intervals of the rainfall event 1 d after fertilizer application (The insets show the runoff losses from Str and control treatments), b) The runoff losses of P from the treatments during the 30-min rain events performed 3, 7, 14 and 21 d after fertilizer application. Error bars represent the standard deviation (n=3) and different letters indicate statistical significance ($P \leq 0.05$).

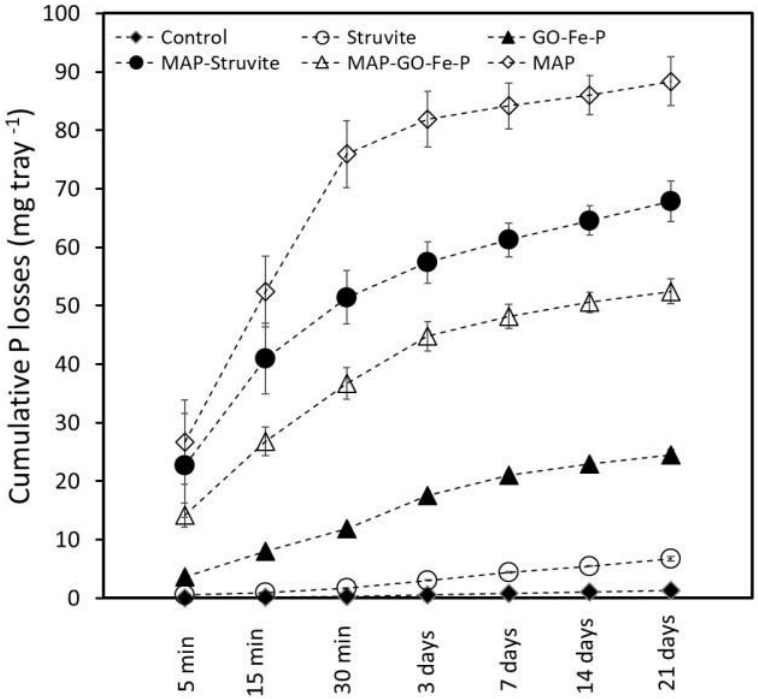

Figure 4. The cumulative runoff losses of dissolved P from fertilizers across the rainfall events, reported as milligrams of P per tray. Error bars represent the standard deviation (n=3).

The higher runoff P losses of the MAP-Str than MAP-GO-Fe-P, despite the low solubility of Str, can perhaps be explained by the structural characteristic and hardness of the granules. Although both fertilizers were made by mixing the same MAP powder with slow release sources, and the same pressure was used during manufacture, the crushing strength of the MAP-GO-Fe-P granules was significantly higher (54.5 ±5.5 N) than those of MAP-Str (10.9±3.3 N), Fig. S6. As illustrated in Fig. 5, during compression, loosely packed particles transform and rotate at relatively low contact deformations. Subsequently, due to the increase in the elastic-plastic contact stresses, some particles deform and break, and smaller particles tend to fill the pores to make the final granule. Several studies[70, 71] have shown that different factors and particle properties including powder flowability, particle size distribution, shape and hardness can influence the compression behaviour of powders and the strength of the final granule. Graphene oxide-based materials, due to their unique properties including planar structure and the flexibility of sheets, can fill pores between the MAP particles and may have conferred higher granule strength to the MAP-GO-Fe-P treatment, and therefore perhaps reducing granule degradation by rainfall impact and reducing runoff losses. Several studies have demonstrated the effect of graphene and its derivatives on enhancing the mechanical properties of alloys, cement and fertilizers.[72-74] Furthermore, Shigaki et al.[75] found that rainfall intensity and P solubility can influence P transport in runoff. Therefore, fertilizers with low mechanical strength are more affected under the rainfall intensity which can influence P transport in runoff. The SEM images (Fig. 5 g-j) from the surface of the both types of dual-release granules confirmed our hypothesis that

MAP-GO-Fe-P granules were more compacted than MAP-Str granules. Large residues of undissolved MAP-GO-Fe-P with preserved original shape were also detected at the end of the runoff event, further supporting our hypothesis (Fig. S7).

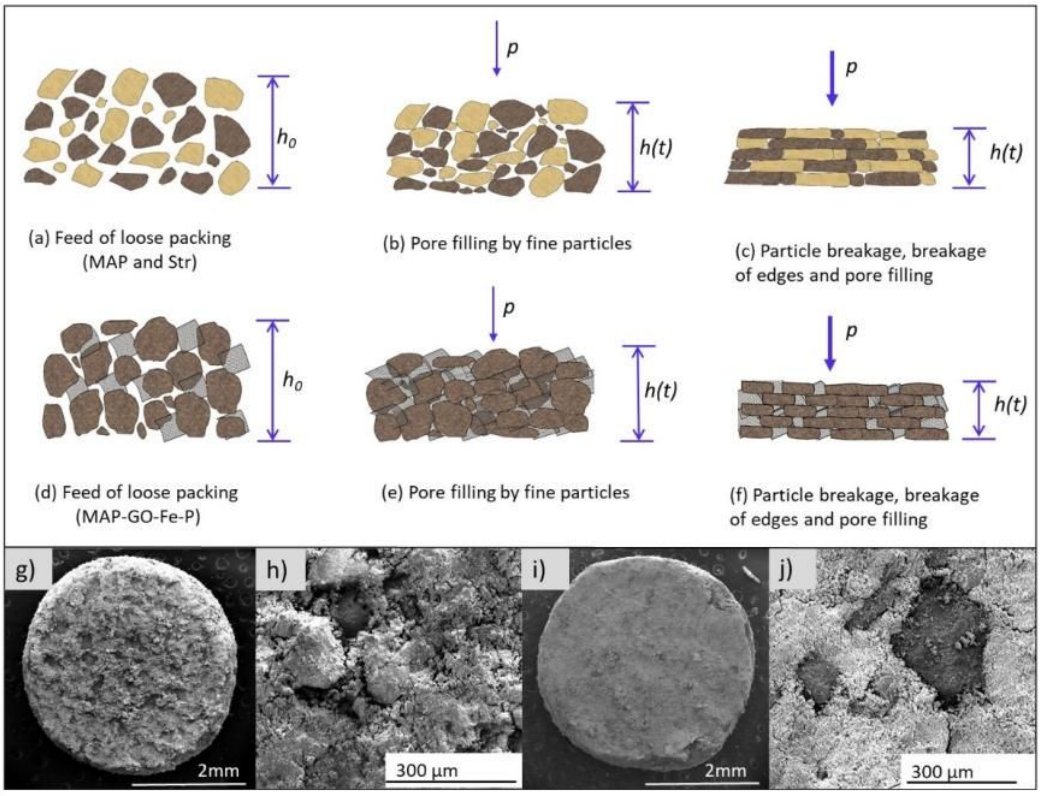

Figure 5. Schematic of micro-process and formation of MAP-Str and MAP-GO-Fe-P a) Feed of loose particles of MAP and Str are subjected to the pressure, b) Fine particles are moving and fill the pores between the larger particles, c) Particles and their edges tend to break and gaps between the pores are filled, d) Feed of loose particles of MAP and GO-Fe-P sheets, e) Fine MAP particles and GO-Fe-P sheets rearranged to fill the gaps between MAP particles, f) MAP particles and their edges tend to break and GO-Fe-P sheets fill the pores and gaps between the MAP particles, g) and h) Low and high magnification SEM images of dual- release MAP-Str and i) and j) Low and high magnification SEM images of dual- release MAP-GO-Fe-P.

Diffusion of P into soil

At any given time, the diffusion of P from MAP granules was higher than all other treatments in MO soil (Fig. 6a). The P diffusion zone visualized around the granule was smaller for the slow- release fertilizers (Str and GO-Fe-P) in MO soils compared to other treatments while GO-Fe-P was superior to Str. In MO soil, there was little difference in visualized P diffusion between granules containing slow and fast release P. The diffusion of P from both dual-release fertilizers steadily increased until 21 d of incubation but enhanced slightly or was at the same level for 28 d showing the P release was governed

by slow release source after 21 d. In the sandy soil low in Al and Fe (MC), the P released from MAP diffused very quickly and reached the border of the Petri dish by the third day of incubation, due to the low P buffering capacity of the soil (Fig. 6b).[76] Released P from dual-release fertilizers diffused in soil very quickly and reached the border of incubated dish in a week. Struvite fertilizers had the lowest diffusion compared to all other fertilizers.

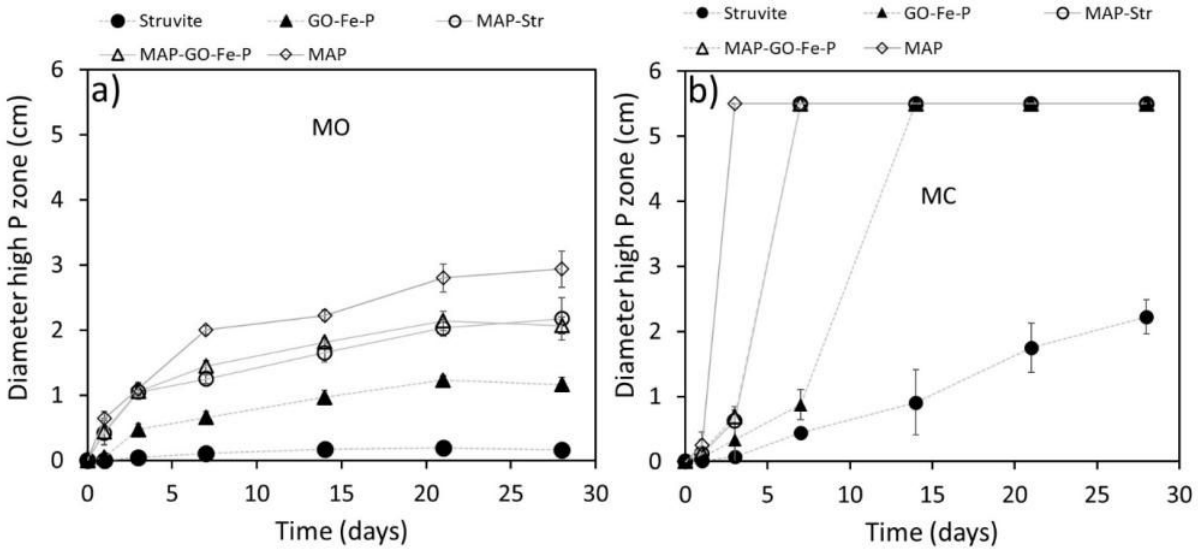

Figure 6. a) Diameter of the high-P zone in Monarto soil and b) Mt Compass soil from the treatments at 1, 3, 7, 14, 21 and 28 d after the addition of fertilizers. Error bars represent the standard deviation (n=3).

Chemical analysis of soil at the end of the incubation confirmed the findings from the visualization experiment. It was very clear that most of the P remained in the inner section at the end of the 4-week incubation for Str and GO-Fe-P granules (Fig. 7a and b) in both soils. However, higher % of P recovered from Str compared to GO-Fe-P at <8mm was most likely related to the incomplete dissolution of Str. The amount of P extracted from the >8 mm section increased for dual-release granules compared to their related slow-release formulation and the fraction of P recovered at >8 mm for MAP-Str was lower than MAP-GO-Fe-P.

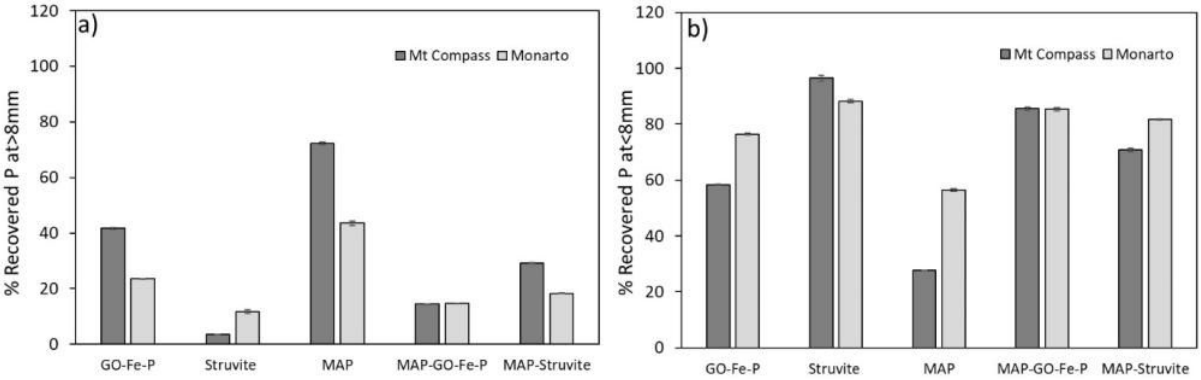

Figure 7. The percentage of P recovered by acid from treatments incubated in Monarto and Mt Compass soils for 28 d at a) >8 mm and b) <8mm. Error bars represent the standard deviation (n=3)

Phosphorus leaching

The cumulative dissolved P leachate from the soil column is presented in Fig. 8a. It is clearly observed that an average of 37 mg of P was leached from the column containing MAP after 1 d which corresponded to the 62% of the applied P. The amount of P leached from the MAP fertilizers was 57.5 mg by 3 d corresponding to 97% of P initially present in the column. In comparison, the amount of P leached was 31 mg for the MAP-GO-Fe-P and 25 mg for the columns containing MAP-Str, corresponding to 52 and 41% of the P applied as dual-release fertilizer, respectively. MAP-GO-Fe-P showed higher cumulative loss than the MAP-Str treatment except for the initial leaching events (1 and 3 d) where P losses were most likely related to the highly soluble part of the fertilizer treatment. The amount of P leached from the column containing GO-Fe-P was around 6% for the first day of incubation and it reached up to 18% at the end of the leaching event. In contrast, the leachates for the Str were more gradual over time, as there was less difference in P loss between the different leaching events resulting in only 3.5% of added P to the columns leached over the whole experiment.

Many sandy soils are often P deficient with less aluminium and iron based minerals that can adsorb P.[4] rapid transport in sandy soils and low P-retention capacity may result in large P leaching.[4, 77] The amount of P loss from the columns is also related to the fertilizer source. The high P loss from MAP was related to its high solubility. Fertilizers with slow-release properties produced the least P lost during leaching experiments. It has been reported that P release is very quick from water-soluble P fertilizer granules with most of the P leaving the granules within days, [78] hence the leaching of all P from MAP by 3 d. The results of the leaching study was in good agreement with the results of the Petri dish incubation investigation.

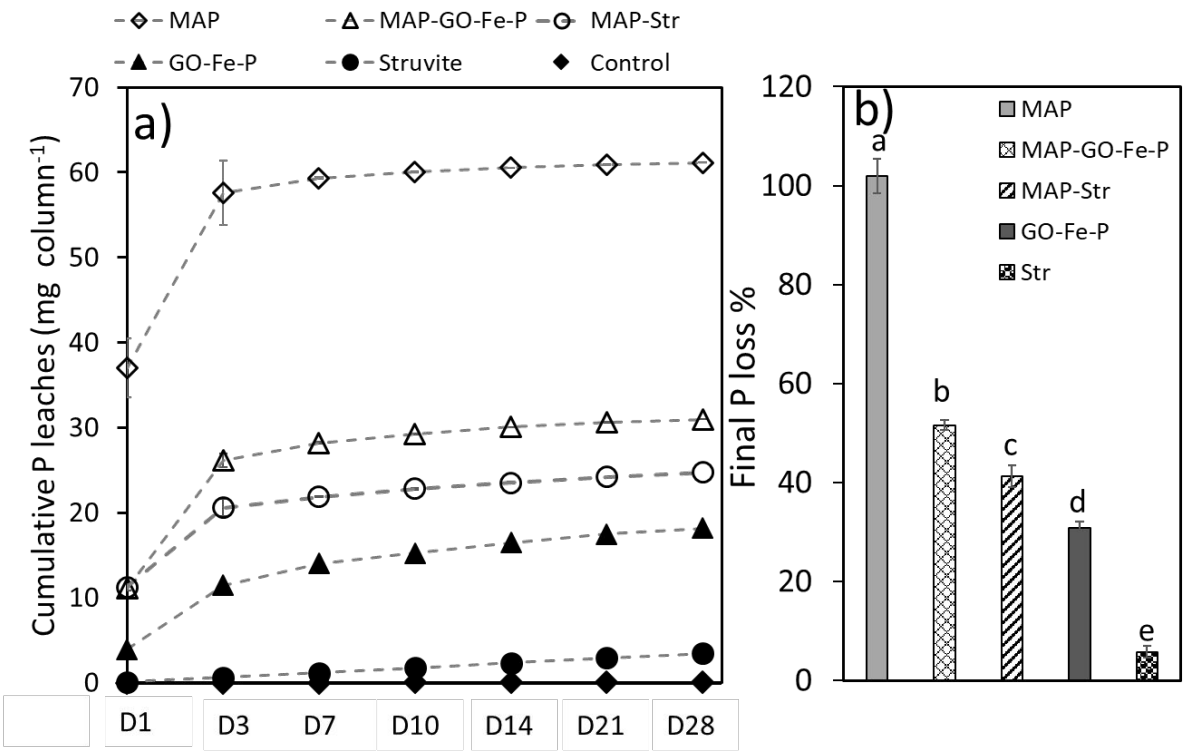

Figure 8. a) Cumulative leaching of the dissolved P from all fertilizers across the leaching events of 1, 3, 7, 15 and 28 days, reported as mg of P per treatment, and b) The total % of leached P from MAP, GO-Fe-P, MAP-GO-Fe-P and MAP-Str at the end of leaching event. Error bars represent the standard deviation (n=3) and different letters indicate statistical significance ($P \leq 0.05$).

A possible drawback of the application of GO composites as fertilizers could be the higher toxicity of GO compared to other alternative nanomaterials, such as clays.[79] Dimiev et al. [64] have found that 'prolonged exposure of GO to water gradually degrades GO flakes, converting them into humic acid-like structures'. Although degradation of GO applied as fertilizer to humic acid-like structures could improve soil quality, the kinetics of this degradation might be too slow to prevent possible toxicity of GO. A more detailed knowledge of GO toxicity in soil is necessary before large-scale application of GO composites as fertilizers.

Conclusions

The environmental issues associated with losses of P in runoff and leaching from highly soluble P fertilizers, coupled with the low agronomic effectiveness of very insoluble P sources, led to the preparation of dual release P fertilizers by co-compaction of both soluble (MAP) and slow release P sources (struvite and graphene composites). It is evident that dual-release P products can indeed be formulated that have P release patterns, P leaching and P runoff losses that are intermediate between highly soluble products and slowly soluble materials. These dual-release products may offer an

opportunity to reduce the environmentally damaging losses of P that can occur immediately after fertilizer application, while at the same time providing a sufficient rate of P supply to crops so that agronomic effectiveness is not compromised. Further research is needed to define the agronomic effectiveness of dual-release products for a range of crops and on soils differing in the P supply.

Supporting information: XRD spectra of the GO-3Fe, GO-4Fe, GO-5Fe, GO-3Fe-P, GO-4Fe-P, and GO-5Fe-P composites, FTIR spectra of GO-3Fe, GO-4Fe, GO-5Fe, GO-3Fe-P, GO-4Fe-P, and GO-5Fe-P composites, TGA spectra of GO-3Fe, GO-4Fe, GO-5Fe, GO-3Fe-P, GO-4Fe-P, and GO-5Fe-P composites, kinetics of P, K, and S release from GO-3Fe-P composite, granular crushing strength of MAP-GO-3Fe-P and MAP-Str granules, photos of GO-3Fe-P and MAP-GO-3Fe-P granules, SEM of GO-3Fe-P and MAP-GO-3Fe-P granules.

Acknowledgment: The authors express their appreciation for the financial support of this study by The Mosaic Company and the Australian Research Council (Discovery Project DP1501001760 and Project IH 150100003, ARC Research Hub for Graphene Enabled Industry Transformation). The authors thank Colin Rivers, Bogumila Tomczak and Ashleigh Broadbent for the assistance with runoff and leaching experiments, and ICP-OES analysis and Dr Diana Tran for taking AFM image of GO.

References:

1. *Phosphorus: Agriculture and the environment*. American Society of Agronomy, Crop Science Society of America, and Soil Science Society of America: Madison, WI, 2005.
2. Meinikmann, K.; Hupfer, M.; Lewandowski, J., Phosphorus in groundwater discharge – A potential source for lake eutrophication. *J. Hydrol.* **2015,** 524, 214-226.
3. Everaert, M.; da Silva, R. C.; Degryse, F.; McLaughlin, M. J.; Smolders, E., Limited dissolved phosphorus runoff losses from layered double hydroxide and struvite fertilizers in a rainfall simulation study. *J. Environ. Qual.* **2018,** 47, (2), 371-377.
4. Alleoni, L. R. F.; Brinton, S. R.; O'Connor, G. A., Runoff and leachate losses of phosphorus in a sandy spodosol amended with biosolids. *J. Environ. Qual.* **2008,** 37, (1), 259-265.
5. Hart, M. R.; Quin, B. F.; Nguyen, M. L., Phosphorus runoff from agricultural land and direct fertilizer effects. *J. Environ. Qual.* **2004,** 33, (6), 1954-1972.
6. Kumaragamage, D.; Flaten, D.; Akinremi, O. O.; Sawka, C.; Zvomuya, F., Soil test phosphorus changes and phosphorus runoff losses in incubated soils treated with livestock manures and synthetic fertilizer. *Can. J. Soil Sci.* **2011,** 91, (3), 375-384.
7. McDowell, R. W.; Littlejohn, R. P.; Blennerhassett, J. D., Phosphorus fertilizer form affects phosphorus loss to waterways: a paired catchment study. *Soil Use and Manage.* **2010,** 26, (3), 365-373.
8. Nash, D. M.; McDowell, R. W.; Condron, L. M.; McLaughlin, M. J., Direct exports of phosphorus from fertilizers applied to grazed pastures. *J. Environ. Qual.* **2019,** 48, (5), 1380-1396.
9. Timilsena, Y. P.; Adhikari, R.; Casey, P.; Muster, T.; Gill, H.; Adhikari, B., Enhanced efficiency fertilisers: a review of formulation and nutrient release patterns. *J. Sci. Food Agr.* **2015,** 95, (6), 1131-1142.

10. Wu, L.; Liu, M., Preparation and properties of chitosan-coated NPK compound fertilizer with controlled-release and water-retention. *Carbohydr. Polym.* **2008,** 72, (2), 240-247.
11. Ibrahim, A. A.; Jibril, B. Y., Controlled release of paraffin wax/rosin-coated fertilizers. *Ind. Eng. Chem. Res.* **2005,** 44, (7), 2288-2291.
12. Tomaszewska, M.; Jarosiewicz, A., Use of polysulfone in controlled-release NPK fertilizer formulations. *J. Agric. Food Chem.* **2002,** 50, (16), 4634-4639.
13. Liang, R.; Liu, M.; Wu, L., Controlled release NPK compound fertilizer with the function of water retention. *React. Funct. Polym.* **2007,** 67, (9), 769-779.
14. Adams, C.; Frantz, J.; Bugbee, B., Macro- and micronutrient-release characteristics of three polymer-coated fertilizers: Theory and measurements. *J. Plant Nutr. Soil Sci.* **2013,** 176, (1), 76-88.
15. Fertahi, S.; Bertrand, I.; Ilsouk, M.; Oukarroum, A.; Amjoud, M. B.; Zeroual, Y.; Barakat, A., New generation of controlled release phosphorus fertilizers based on biological macromolecules: Effect of formulation properties on phosphorus release. *Int. J. Biol. Macromol.* **2020,** 143, 153-162.
16. Trenkel, M. E., *Slow and Controlled-Release and Stabilized Fertilizers*. International Fertilizer Industry Association, Paris, France (2010): 2010.
17. Briassoulis, D.; Dejean, C., Critical review of norms and standards for biodegradable agricultural plastics part I. Biodegradation in Soil. *J. Polym. Environ.* **2010,** 18, (3), 384-400.
18. Montalvo, D.; McLaughlin, M. J.; Degryse, F., Efficacy of hydroxyapatite nanoparticles as phosphorus fertilizer in andisols and oxisols. *Soil Sci. Soc. Am. J.* **2015,** 79, (2), 551-558.
19. Degryse, F.; Baird, R.; da Silva, R. C.; McLaughlin, M. J., Dissolution rate and agronomic effectiveness of struvite fertilizers – effect of soil pH, granulation and base excess. *Plant Soil* **2016**, 1-14.
20. Nieminen, M., Properties of slow-release phosphorus fertilizers with special reference to their use on drained peatland forests. A review. *Suo* **1997,** 48, (4), 115-126.
21. Everaert, M.; Degryse, F.; McLaughlin, M. J.; De Vos, D.; Smolders, E., Agronomic effectiveness of granulated and powdered P-exchanged Mg–Al LDH relative to struvite and MAP. *J. Agric. Food Chem.* **2017,** 65, (32), 6736-6744.
22. Bernardo, M. P.; Guimarães, G. G. F.; Majaron, V. F.; Ribeiro, C., Controlled release of phosphate from layered double hydroxide structures: Dynamics in soil and application as smart fertilizer. *ACS Sustainable Chem. Eng.* **2018,** 6, (4), 5152-5161.
23. Bhardwaj, D.; Sharma, M.; Sharma, P.; Tomar, R., Synthesis and surfactant modification of clinoptilolite and montmorillonite for the removal of nitrate and preparation of slow release nitrogen fertilizer. *J. Hazard. Mater.* **2012,** 227-228, 292-300.
24. Kabiri, S.; Degryse, F.; Tran, D. N. H.; da Silva, R. C.; McLaughlin, M. J.; Losic, D., Graphene Oxide: A New Carrier for Slow Release of Plant Micronutrients. *ACS Appl. Mater. Interfaces* **2017,** 9, (49), 43325-43335.
25. Shaviv, A.; Mikkelsen, R. L., Controlled-release fertilizers to increase efficiency of nutrient use and minimize environmental degradation - A review. *Fert. Res.* **1993,** 35, (1), 1-12.
26. Antonini, S.; Arias, M. A.; Eichert, T.; Clemens, J., Greenhouse evaluation and environmental impact assessment of different urine-derived struvite fertilizers as phosphorus sources for plants. *Chemosphere* **2012,** 89, (10), 1202-1210.
27. Cabeza, R.; Steingrobe, B.; Römer, W.; Claassen, N., Effectiveness of recycled P products as P fertilizers, as evaluated in pot experiments. *Nutr. Cycl. Agroecosys.* **2011,** 91, (2), 173.
28. Bolland, M. D. A.; Gilkes, R. J., Reactive rock phosphate fertilizers and soil testing for phosphorus: The effect of particle size of the rock phosphate. *Fert. Res.* **1989,** 21, (2), 75-93.
29. Andelkovic, I. B.; Kabiri, S.; da Silva, R. C.; Tavakkoli, E.; Kirby, J. K.; Losic, D.; McLaughlin, M. J., Optimisation of phosphate loading on graphene oxide–Fe(iii) composites – possibilities for engineering slow release fertilisers. *New J. Chem.* **2019,** 43, (22), 8580-8589.
30. da Silva, R. C.; Baird, R.; Degryse, F.; McLaughlin, M. J., Slow and fast-release boron sources in potash fertilizers: Spatial variability, nutrient dissolution and plant uptake. *Soil Sci. Soc. Am. J.* **2018,** 82, (6), 1437-1448.

31. Andelkovic, I. B.; Kabiri, S.; Tavakkoli, E.; Kirby, J. K.; McLaughlin, M. J.; Losic, D., Graphene oxide-Fe(III) composite containing phosphate – A novel slow release fertilizer for improved agriculture management. *J. Clean. Prod.* **2018,** 185, 97-104.
32. Shih, C.-J.; Lin, S.; Sharma, R.; Strano, M. S.; Blankschtein, D., Understanding the pH-dependent behavior of graphene oxide aqueous solutions: A comparative experimental and molecular dynamics simulation study. *Langmuir* **2012,** 28, (1), 235-241.
33. Zhang, K.; Dwivedi, V.; Chi, C.; Wu, J., Graphene oxide/ferric hydroxide composites for efficient arsenate removal from drinking water. *J. Hazard. Mater.* **2010,** 182, (1), 162-168.
34. Marcano, D. C.; Kosynkin, D. V.; Berlin, J. M.; Sinitskii, A.; Sun, Z.; Slesarev, A.; Alemany, L. B.; Lu, W.; Tour, J. M., Improved synthesis of graphene oxide. *ACS Nano* **2010,** 4, (8), 4806-4814.
35. Zarcinas, B. A.; McLaughlin, M. J.; Smart, M. K., The effect of acid digestion technique on the performance of nebulization systems used in inductively coupled plasma spectrometry. *Commun. Soil Sci. Plant Anal.* **1996,** 27, (5-8), 1331-1354.
36. Baird, R.; da Silva, R. C.; Degryse, F.; McLaughlin, M. J., A column perfusion test to assess the kinetics of nutrient release by soluble, sparingly soluble and coated granular fertilizers. *J. Plant Nutr. Soil Sci.* 0, (0).
37. Matejovic, I., Determination of carbon and nitrogen in samples of various soils by the dry combustion. *Commun. Soil Sci. Plant Anal.* **1997,** 28, (17-18), 1499-1511.
38. Martin, A. E.; Reeve, R., A rapid manometic method for determining soil carbonate Soil Sci. **1955,** 79, (3), 11.
39. McKenzie, N.; Coughlan, K.; Cresswell, H., *Soil physical measurements and interpretation for land evaluation.* CSIRO Publishing, Collingwood 2002.
40. Rayment, G. E., *Australian laboratory handbook of soil and water chemical methods / G.E. Rayment and F.R. Higginson*. Inkata Press: Melbourne, 1992.
41. Degryse, F.; McLaughlin, M. J., Phosphorus diffusion from fertilizer: Visualization, chemical measurements, and modeling. *Soil Sci. Soc. Am. J.* **2014,** 78, (3), 832-842.
42. Lombi, E.; McLaughlin, M. J.; Johnston, C.; Armstrong, R. D.; Holloway, R. E., Mobility, solubility and lability of fluid and granular forms of P fertiliser in calcareous and non-calcareous soils under laboratory conditions. *Plant Soil* **2005,** 269, (1), 25-34.
43. Dash, S.; Murthy, P. N.; Nath, L.; Chowdhury, P., Kinetic modeling on drug release from controled drug delivery systems *Acta Polon. Pharm.* **2010,** 67, (3), 16.
44. Sempeho, S. I.; Kim, H. T.; Mubofu, E.; Hilonga, A., Meticulous overview on the controlled release fertilizers. *Adv. Chem.* **2014,** 2014, 16.
45. Jeong, H.-K.; Lee, Y. P.; Lahaye, R. J. W. E.; Park, M.-H.; An, K. H.; Kim, I. J.; Yang, C.-W.; Park, C. Y.; Ruoff, R. S.; Lee, Y. H., Evidence of graphitic AB stacking order of graphite oxides. *J. Am. Chem. Soc.* **2008,** 130, (4), 1362-1366.
46. Dong, Y.; Li, J.; Shi, L.; Xu, J.; Wang, X.; Guo, Z.; Liu, W., Graphene oxide-iron complex: synthesis, characterization and visible-light-driven photocatalysis. *J. Mat. Chem. A* **2013,** 1, (3), 644-650.
47. Zhang, Q.; Lin, N.; Xu, T.; Shen, K.; Li, T.; Han, Y.; Zhou, J.; Qian, Y., Scalable synthesis of carbon stabilized SiO/graphite sheets composite as anode for high-performance Li ion batteries. *RSC Adv.* **2017,** 7, (63), 39762-39766.
48. Hontoria-Lucas, C.; López-Peinado, A. J.; López-González, J. d. D.; Rojas-Cervantes, M. L.; Martín-Aranda, R. M., Study of oxygen-containing groups in a series of graphite oxides: Physical and chemical characterization. *Carbon* **1995,** 33, (11), 1585-1592.
49. Sitko, R.; Turek, E.; Zawisza, B.; Malicka, E.; Talik, E.; Heimann, J.; Gagor, A.; Feist, B.; Wrzalik, R., Adsorption of divalent metal ions from aqueous solutions using graphene oxide. *Dalton Trans.* **2013,** 42, (16), 5682-5689.
50. Acik, M.; Lee, G.; Mattevi, C.; Pirkle, A.; Wallace, R. M.; Chhowalla, M.; Cho, K.; Chabal, Y., The role of oxygen during thermal reduction of graphene oxide studied by infrared absorption spectroscopy. *J. Phys. Chem. C* **2011,** 115, (40), 19761-19781.

51. Guo, H.-L.; Wang, X.-F.; Qian, Q.-Y.; Wang, F.-B.; Xia, X.-H., A green approach to the synthesis of graphene nanosheets. *ACS Nano* **2009,** 3, (9), 2653-2659.
52. Kabiri, S.; Tran, D. N. H.; Altalhi, T.; Losic, D., Outstanding adsorption performance of graphene–carbon nanotube aerogels for continuous oil removal. *Carbon* **2014,** 80, 523-533.
53. Kabiri, S.; Tran, D. N. H.; Azari, S.; Losic, D., Graphene-diatom silica aerogels for efficient removal of mercury ions from water. *ACS Appl. Mater. Interfaces* **2015,** 7, (22), 11815-11823.
54. Tran, D. N. H.; Kabiri, S.; Losic, D., A green approach for the reduction of graphene oxide nanosheets using non-aromatic amino acids. *Carbon* **2014,** 76, 193-202.
55. Chandra, V.; Park, J.; Chun, Y.; Lee, J. W.; Hwang, I.-C.; Kim, K. S., Water-dispersible magnetite-reduced graphene oxide composites for arsenic removal. *ACS Nano* **2010,** 4, (7), 3979-3986.
56. Persson, P.; Nilsson, N.; Sjöberg, S., Structure and bonding of orthophosphate ions at the Iron oxide–aqueous interface. *J. Colloid Interface Sci.* **1996,** 177, (1), 263-275.
57. Tran, D. N. H.; Kabiri, S.; Wang, L.; Losic, D., Engineered graphene-nanoparticle aerogel composites for efficient removal of phosphate from water. *J. Mater Chem. A* **2015,** 3, (13), 6844-6852.
58. Hsiao, M.-C.; Ma, C.-C. M.; Chiang, J.-C.; Ho, K.-K.; Chou, T.-Y.; Xie, X.; Tsai, C.-H.; Chang, L.-H.; Hsieh, C.-K., Thermally conductive and electrically insulating epoxy nanocomposites with thermally reduced graphene oxide-silica hybrid nanosheets. *Nanoscale* **2013,** 5, (13), 5863-5871.
59. Zhang, L.; Schlesinger, M. E.; Brow, R. K., Phase equilibria in the Fe2O3–P2O5 system. *J. Am. Ceram. Soc.* **2011,** 94, (5), 1605-1610.
60. Gurunathan, S.; Woong Han, J.; Kim, E.; Kwon, D.-N.; Park, J.-K.; Kim, J.-H., Enhanced green fluorescent protein-mediated synthesis of biocompatible graphene. *J. Nanobiotechnol.* **2014,** 12, (1), 41.
61. Lin, T.-Y.; Chen, D.-H., One-step green synthesis of arginine-capped iron oxide/reduced graphene oxide nanocomposite and its use for acid dye removal. *RSC Adv.* **2014,** 4, (56), 29357-29364.
62. Ryden, J. C.; Syers, J. K.; Tillman, R. W., Inorganic anion sorption and interactions with phosphate sorption by hydrous ferric oxide gel. *J. Soil Sci.* **1987,** 38, (2), 211-217.
63. Khalil, A. M. E.; Eljamal, O.; Amen, T. W. M.; Sugihara, Y.; Matsunaga, N., Optimized nano-scale zero-valent iron supported on treated activated carbon for enhanced nitrate and phosphate removal from water. *Chem. Eng. J.* **2017,** 309, 349-365.
64. Dimiev, A. M.; Alemany, L. B.; Tour, J. M., Graphene oxide. Origin of acidity, its instability in water, and a new dynamic structural model. *ACS Nano* **2013,** 7, (1), 576-588.
65. Dong, Y.; Li, J.; Shi, L.; Xu, J.; Wang, X.; Guo, Z.; Liu, W., Graphene oxide–iron complex: synthesis, characterization and visible-light-driven photocatalysis. *J. Mat. Chem. A* **2013,** 1, (3), 644-650.
66. Bhuiyan, M. I. H.; Mavinic, D. S.; Beckie, R. D., A solubility anf thermodynamic study of struvite. *Environ. Technol.* **2007,** 28, (9), 1015-1026.
67. Mario, G.; Gabriele, G., Mathematical modelling and controlled drug delivery: Matrix systems. *Curr. Drug Delivery* **2005,** 2, (1), 97-116.
68. Dash, S.; Murthy, P. N.; Nath, L.; Chowdhury, P., Kinetic modeling on drug release from controlled drug delivery systems. *Acta Pol Pharm. 2010;67(3):217–223.* **2010,** 67(3), 217–223.
69. Wang, W.; Liang, T.; Wang, L.; Liu, Y.; Wang, Y.; Zhang, C., The effects of fertilizer applications on runoff loss of phosphorus. *Environ. Earth Sci.* **2013,** 68, (5), 1313-1319.
70. Marigo, M.; Cairns, D. L.; Bowen, J.; Ingram, A.; Stitt, E. H., Relationship between single and bulk mechanical properties for zeolite ZSM5 spray-dried particles. *Particuology* **2014,** 14, 130-138.
71. Stasiak, M.; Tomas, J.; Molenda, M.; Rusinek, R.; Mueller, P., Uniaxial compaction behaviour and elasticity of cohesive powders. *Powder Technol.* **2010,** 203, (3), 482-488.
72. Gholampour, A.; Valizadeh Kiamahalleh, M.; Tran, D. N. H.; Ozbakkaloglu, T.; Losic, D., From graphene oxide to reduced graphene oxide: Impact on the physiochemical and mechanical properties of graphene–cement composites. *ACS Appl. Mater. Interfaces* **2017,** 9, (49), 43275-43286.

73. Li, Z.; Guo, Q.; Li, Z.; Fan, G.; Xiong, D.-B.; Su, Y.; Zhang, J.; Zhang, D., Enhanced mechanical properties of graphene (reduced graphene oxide)/aluminum composites with a bioinspired nanolaminated structure. *Nano Lett.* **2015,** 15, (12), 8077-8083.
74. Kabiri, S.; Baird, R.; Tran, D. N. H.; Andelkovic, I.; McLaughlin, M. J.; Losic, D., Cogranulation of low rates of graphene and graphene oxide with macronutrient fertilizers remarkably improves their physical properties. *ACS Sustainable Chem. Eng.* **2018,** 6, (1), 1299-1309.
75. Shigaki, F.; Sharpley, A.; Prochnow, L. I., Rainfall intensity and phosphorus source effects on phosphorus transport in surface runoff from soil trays. *Sci. Total Environ.* **2007,** 373, (1), 334-343.
76. Degryse, F.; Baird, R.; da Silva, R. C.; McLaughlin, M. J., Dissolution rate and agronomic effectiveness of struvite fertilizers – effect of soil pH, granulation and base excess. *Plant Soil* **2017,** 410, (1), 139-152.
77. Djodjic, F.; Börling, K.; Bergström, L., Phosphorus leaching in relation to soil type and soil phosphorus content. *J. Environ. Qual.* **2004,** 33, (2), 678-684.
78. McLaughlin, M. J.; McBeath, T. M.; Smernik, R.; Stacey, S. P.; Ajiboye, B.; Guppy, C., The chemical nature of P accumulation in agricultural soils—implications for fertiliser management and design: an Australian perspective. *Plant Soil* **2011,** 349, (1), 69-87.
79. Kryuchkova, M.; Danilushkina, A.; Lvov, Y.; Fakhrullin, R., Evaluation of toxicity of nanoclays and graphene oxide in vivo: a Paramecium caudatum study. *Environ. Sci.: Nano* **2016,** 3, (2), 442-452.

For Table of Contents Only